

Modelling and Analysis of Hysteresis in Piezoelectric Actuator

A.K. Singh¹ and Deepak Apte²

¹Defence Institute of Advanced Technology, Pune-411 025

²Indian Institute of Science, Bangalore-560 012

ABSTRACT

Piezoelectric actuators are the potential actuators having a wide range of applications in smart structures and systems. However, the presence of hysteresis nonlinearity leads to degradation in their performance. This paper discusses a mathematical model for hysteresis in piezoelectric actuators based on domain wall bending and translation¹. The validity of the model has been illustrated through comparison with the experimental observations of piezoelectric stack actuator developed using PZT5H material.

Keywords: Piezoelectric, hysteresis, polarisation, domain wall

NOMENCLATURE

$a(=E_o/3T_c)$	Incorporate relative thermal effects	n	Average density of pinning sites
c	Reversible coefficient	N	Number of dipole moments
d	Point charge separation	P	Polarisation
d_{jm}	Piezoelectric coefficient tensor	P_{an}	Anhysteretic polarisation
D_e	Electric displacement	P_{rev}	Reversible polarisation
E	Electric field	P_{irrv}	Irreversible polarisation
E_e	Effective electric field	P'	Applied pressure
E_o	Scaling electric field constant	P_s	Saturation polarisation
F	Force	P_{total}	Total polarisation
g_{33}	Piezoelectric voltage constant tensor	P_o	Biasing polarisation
i_s	Polarisation switching current	p	Dipole moment
k	Average energy required to break pinning site	Q	Electric charge
K_B	Boltzmann's constant	r	Radius of curvature
		s_{33}	Elastic compliance tensor

S_{33}	Strain tensor
T_3	Stress tensor
T	Operating temperature
T_c	Curie temperature constant
ε	Potential energy
ε_{pin}	Energy required to break pinning site
σ	Stress
β_{33}	Dielectric permeability
$\varphi(p)$	Polarisation switching rate
α	Quantifies domain interaction
$\Delta\varepsilon$	Change in energy per unit volume
χ	Susceptibility
χ_{in}	Initial differential susceptibility
χ_{an}	Differential susceptibility at origin
χ_m^+ & χ_m^-	Differential susceptibility before & after field reversal at tip
χ_r & χ_r	Differential susceptibility at + ve and - ve remanence points
χ_e	Differential susceptibility at coercive field

1. INTRODUCTION

Piezoelectric actuators are useful in defence, as well as, in industrial applications for small deflection positioning system because of a number of advantages. However, their major limitation is hysteresis nonlinearity inherently present in input-output behaviour, which resulted in lack of accuracy in control system and ultimately led to degradation in their performance^{1,2}. The maximum error was about 10-15 per cent of path covered for piezoelectric actuators in open-loop control system. Reliable prediction of actuator output, considering the hysteresis, would be a valuable tool when piezoelectric actuator is employed as a part of control system. To overcome the nonlinear hysteresis, it must be ascertained and eventually quantified.

In an effort to provide a model, incorporating the aspects of underlying physical mechanism, theory of piezoelectric hysteresis has been considered, which is based on domain wall dynamics and quantification of energy losses due to internal inclusions in the material^{3,4}. The model presented here follows three steps, first, constitutive relations were obtained through consideration of Langevin, Ising spin model with domain interaction incorporated through mean field relations which yielded an anhysteretic model. In the second step, hysteresis is incorporated through consideration of domain wall dynamics and quantification of energy losses due to inherent inclusions of pinning sites within the material. In the third step, parameter determination has been done.

2. HYSTERESIS MODELLING

Takacs⁵ has discussed the evolution of various models used for hysteresis. The nature of hysteresis models for piezoceramic material can be roughly categorised into three categories, (i) microscopic theories based on quantum mechanics, classical elasticity, (ii) macroscopic theories based on phenomenological concepts, and (iii) semi-macroscopic theories, which are derived using a combination of two approaches. These theories are discussed here.

2.1 Microscopic Theory

Microscopic theory has described the previous polarisation process at domain level, and is based on a theory, which represented energy as a function of polarisation and temperature. Kuebler⁶ has shown that polarisation and electric field can be related to each other and represented as a function of electric field

$$P = f(E, t) \quad (1)$$

which also included various dynamic parameters of polarisation reversal such as switching current, switching time, switching resistance. Drougard⁷ has experimentally shown that polarisation switching current (i_s) is not only dependent on the applied field but also upon state of polarisation of the crystal:

$$i_s = \varphi(p)e^{-\alpha/E} \quad (2)$$

where $\varphi(p)$ has taken into account the back history. One of the important conclusions drawn is that polarisation reversal occurred quite predominantly by domain wall motion. Landaure⁸, *et al.* came out with similar type of conclusions. Nomura⁹, *et al.* have shown that when the polarity of DC field is reversed, domain pattern at first disappeared and then began to appear a new. When electric field is applied along one of the polar directions, the crystal became single domain. Pertsav¹⁰, *et al.* have claimed that there existed inter domain interaction and hence, there is existence of internal fields. Internal field depended upon the polarisation. Hence, effective field is the sum of external and internal fields. It is also shown experimentally that domain changed direction when cyclic electric field was applied. Robert¹¹, *et al.* have shown that domain wall velocity in barium titanate crystal depended upon several factors, like applied electric field, different light conditions, thickness, activation field, humidity, types of electrodes, impurity, etc.

Microscopic models at atomic or lattice level involved a large number of parameters and constants, and hence are often difficult to employ in control design. Secondly, the mechanism of domain configuration and switching process are still not well-understood. Hence, it is difficult at present to put up a model from microscopic point of view.

2.2 Macroscopic Theory

Macroscopic theory can be formulated in terms of external parameters, like electric field, stress, strain, and temperature. Such theories have been employed when underlying physics is difficult to quantify and these models have purely mathematical characterisation^{5,12}.

2.3 Semi-macroscopic Theory

Semi-macroscopic models are based on some of the fundamental concepts put forward by both microscopic theories and macroscopic theories. A hysteresis model is discussed here, which is based on quantification of domain wall movements. The model presented here quantifies the resulting hysteresis

through consideration of energy required to translate domain walls and break pinning site. Due to small number of parameters and physical nature of certain parameters, the model is easily updated³.

3. ANHYSTERETIC MODELLING

One dimensional constitutive laws for piezoceramic material¹³ are:

$$S_3 = s_{33}T_3 + g_{33}P_3 \quad (3)$$

$$E_3 = -g_{33}T_3 + \beta_{33}P_3 \quad (4)$$

The methods for modelling functions which quantifies electric field (E) and polarisation (P) are considered. These models are based on the assumptions of orientations of lattice cells.

3.1 Langevin Model

Assuming that the material is isotropic and the cell orientation can be in any direction, prior number of dipole moments between θ and $\theta + d\theta$ is proportional to surface area, $2\pi\sin\theta d\theta$, on a unit sphere. Using Boltzmann's energy relation, one gets a Langevin relation between field and polarisation⁴ given as

$$P = P_s \left[\coth\left(\frac{Ee}{a}\right) - \left(\frac{a}{Ee}\right) \right] \quad (5)$$

3.2 Ising Spin Model

The second model considered here is Ising spin model⁴, which is derived under the assumption that only two orientations are possible in a given cell, one in the direction of electric field, and other in the direction directly opposite to the field, giving

$$P = P_s \tanh\left(\frac{Ee}{a}\right) \quad (6)$$

3.3 Domain Wall Theory

This theory is based on unimpeded domain wall growth and is considered to be reversible. In this model, hysteresis is incorporated through consideration of energy losses of domain wall pinning sites.

3.3.1 Effect of Pinning Sites

To incorporate hysteresis under constant temperature, one quantifies the reversible and irreversible domain wall dynamics exhibited at pinning sites¹⁴.

This section quantifies energy required to break the pinning sites. A pinning site is broken when sufficient energy is provided to overcome a local energy barrier. A domain configuration provided in Fig.1 is considered. Here two domains are separated by domain wall situated at pinning site. P denotes the dipole moment per unit volume. In the two domains P with P' is assumed to be aligned with effective field, E_e . θ is the angle between the dipole moments.

As per Jiles and Atherton¹⁴, change in energy required to overcome pinning sites, and hence to move domain wall, is proportional to the change in energy required to align magnetic moments with field. Thus, energy required to break pinning site is given as

$$\varepsilon_{pin} = - \int_0^P k dP \quad (7)$$

where

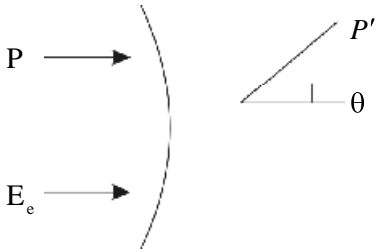


Figure 1. Effect of pinning site.

$$k = \frac{n\varepsilon\pi}{2p} \quad (8)$$

3.3.2 Irreversible Polarisation

The respective polarisation components are denoted as reversible and irreversible polarisation¹⁴.

To characterise irreversible polarisation, polarisation energy for a given effective field can be taken as that observed in ideal case, minus losses necessary to overcome the local energy barriers and hence break pinning sites. Thus irreversible polarisation can be given as

$$\frac{1}{\varepsilon_0} \int_0^{D_e} P_{irr} dD_e = \frac{1}{\varepsilon_0} \int_0^{D_e} P_{an} dD_e - \int_0^{D_e} k \frac{dP_{irr}}{dD_e} dD_e \quad (9)$$

where P_{irr} is the irreversible polarisation, P_{an} is the anhysteretic polarisation, and on differentiation it yields:

$$P_{irr} = P_{an} - \delta\varepsilon_0 k \frac{dP_{irr}}{dE} \quad (10)$$

δ ensures that energy required to break the pinning site always opposes changes in polarisation. To obtain an expression, which facilitates numerical implementation, it can be written as

$$\frac{dP_{irr}}{dE} = \frac{P_{an} - P_{irr}}{\delta k - \alpha(P_{an} - P_{irr})} \quad (11)$$

On solving Eqn (11), irreversible polarisation can be obtained.

3.3.3 Reversible Polarisation

A basic tenet of domain wall theory for piezoelectric material is that wall exhibited bulging and motion¹⁵ and these effects are significant and must be incorporated to obtain an accurate model. The change in energy per unit volume¹⁶ is:

$$\Delta\varepsilon = -PE_e + P_{an}E_e \quad (12)$$

Force on domain wall for fixed field values is then

$$F = \frac{\Delta\varepsilon}{P} \quad (13)$$

To obtain reversible polarisation due to wall movement³, in response to the pressure, displaced volume has to be approximated. The geometry is shown in Fig. 2. The domain wall between the

two pinning sites is considered to be separated by equal distance. The wall is assumed to bow in response to applied pressure (P') with a resulting curvature of radius (r), one has:

$$P' = \frac{2\varepsilon}{r} \quad (14)$$

Assuming that the wall displaces a spherical solid angle, the change in volume is given by

$$\Delta V = \frac{\pi}{6} x(3y^2 + x^2) \quad (15)$$

and simplification yields:

$$P_{rev} = C(P_{an} - P) \quad (16)$$

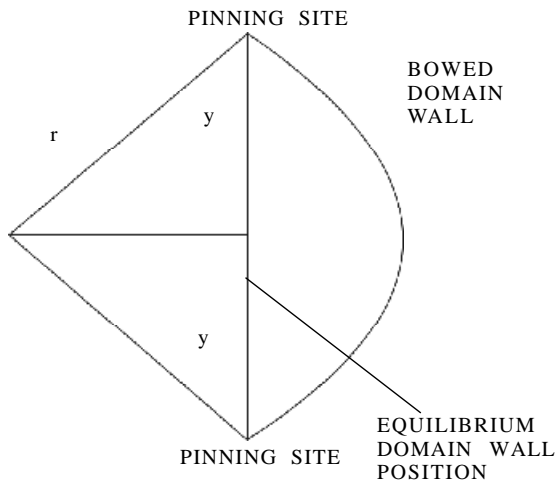


Figure 2. Reversible polarisation.

3.4.4 Total Polarisation

Thus, the total polarisation is given by

$$P = cP_{an} + (1 - c)p_{irr} \quad (17)$$

3.4.5. Parameter Determination

The implementation of model requires determination of five parameters α , a , k , c , P_s for a given material. Here α quantifies the effect of dipole interaction, a incorporates relative thermal effect, k determines average energy required to

break pinning sites, P_s denotes theoretical saturation value beyond which polar interaction prevents further increase in polarisation. The method presented here has used the experimental data for parameter determination¹⁷, using differential susceptibility at various points.

Saturation polarisation (P_s) can be obtained from the available data directly. On differentiation of Eqn (17), on replacing dP_{irr}/dE and on further simplification, one gets:

$$\frac{dP}{dE} = \frac{(1-c)P_{an} - P_{irr}}{k\delta - \alpha(P_{an} - P_{irr})} + c \frac{dP_{an}}{dE} \quad (18)$$

To determine dP/dE , it is necessary to know dP_{an}/dE , the differential susceptibility which is helpful in parameter determination and finally getting results.

$$\frac{dP_{an}}{dE} = P_s \frac{1}{a} \left(a + \alpha \frac{dP}{dE} \right) \left[-\operatorname{csc} h^2 \left(\frac{E_e}{a} \right) + \left(\frac{a}{E_e} \right)^2 \right] \quad (19)$$

3.4.5.1 Initial Susceptibility

Under limits $E \rightarrow 0$, $P_{an} \rightarrow 0$, χ_{an} is differential susceptibility at the origin. From Ising spin model and in the absence of hysteresis, where $E_e = E + \alpha P_{an}$, one has:

$$P = \lim_{\substack{E \rightarrow 0 \\ P \rightarrow 0}} P_s \left[\coth \left(\frac{E_e}{a} \right) - \left(\frac{a}{E_e} \right) \right] \quad (20)$$

$$\text{and } \chi_{an} = \frac{P_s}{3a} (1 + \alpha \chi_{an}) \quad (21)$$

which on solving gives:

$$\chi_{an} = \frac{P_s}{3a - \alpha P_s} \quad (22)$$

$$\alpha = \frac{3a\chi_{an} - P_s}{P_s\chi_{an}} \quad (23)$$

on relating α to a . When field is reversed from

saturation, only change in polarisation is due to reversible effect of polarisation, as $P_{irr} = 0$.

$$P = cP_{an} \quad (24)$$

$$\frac{dP}{dE} = c \frac{dP_{an}}{dE}$$

$$\chi_{in} = \frac{P_s}{3a}(1 + \alpha\chi_{in}) \quad (25)$$

$$a = \frac{P_s}{3\chi_{an}} \quad (26)$$

3.4.5.2 Susceptibility at Field Reversal (E_m, P_m)

The hysteresis loop behaviour at tip value is considered as E_m, P_m . As already stated, when field is first reversed from saturation, the only change in polarisation is due to reversible effects of domain wall. When very close to saturation this can be stated as

$$\frac{dP}{dE} = \frac{dP_{an}}{dE} \quad (27)$$

Let c_m^+ and c_m^- denote the differential susceptibility before and after field reversal at tip loop, one has:

$$c = \frac{\chi_m^-}{\chi_m^+}$$

$$\frac{dP}{dE} = \frac{(1-c)P_{an} - P}{k\delta(1-c) - \alpha(P_{an} - P_{irr})} + c \frac{dP_{an}}{dE} \quad (28)$$

$$\chi_m^+ = \frac{dP_{an}(E_c)}{dE} = \frac{P_{an} - P_m}{k\delta(1-c) - \alpha(P_{an} - P_m)} \quad (29)$$

At remanence, $E=0$, and $P=P_r$, thus

$$\chi_r = (1-c) \frac{P_{an} - P_r}{k\delta(1-c) - \alpha[P_{an}(P_r) - P_r]} + c \frac{dP_{an}(P_r)}{dE} \quad (30)$$

From symmetric Langevin expression, one has:

$$P_{an}(P_r) = P_s \left[\coth\left(\frac{\alpha P_r}{a}\right) - \left(\frac{a}{\alpha P_r}\right) \right] \quad (31)$$

$$\frac{dP_{an}(P_r)}{dE} = \frac{P_s}{a} (1 + \alpha\chi_r) \left[-\operatorname{csc}^2\left(\frac{\alpha P_r}{a}\right) + \left(\frac{a}{\alpha P_r}\right)^2 \right] \quad (32)$$

Using the above equation, initial value of α can be calculated.

3.4.5.3 Coercive Field

At coercive field, $E = E_c$ and $P = 0$, hence differential susceptibility is:

$$\chi_c = \frac{(1-c)P_{an}(E_c)}{k\delta(1-c) - \alpha P_{an}(E_c)} + c \frac{dP_{an}(E_c)}{dE} \quad (33)$$

where $\delta = 1$ and

$$k = P_{an}(E_c) \left(\frac{\alpha}{1-c} + \frac{1}{\chi_c - c \frac{dP_{an}(E_c)}{dE}} \right) \quad (34)$$

For soft material approximating $c = 0$, and $\chi_c = \chi_{an}$, ie., susceptibility at coercive point is approximately equal to slope of the anhysteretic curve at origin

$$k = P_{an}(E_c) \left(\alpha + \frac{1}{\chi_{an}} \right) \text{ as } \chi_c = \chi_{an}, \text{ so} \quad (35)$$

$$P_{an}(E_c) = \chi_{an} E_c \quad (36)$$

hence

$$P_{an}(E_c) = \left(\frac{P_s}{3a - \alpha P_s} \right) E_c \quad (37)$$

On substituting the values of $P_{an}(E_c)$ and χ_{an} in the above equation, one has:

$$k = \frac{E_c}{1 - \frac{\alpha P_s}{3a}} \quad (38)$$

This can be approximated for soft material as

$$k = E_c \quad (39)$$

3.4.5.4 Approximation of χ_{in} and χ_{an}

Calculation of χ_{in} has been done as follows¹⁷:

$$\chi_{in} = \frac{\chi_r^+ + \chi_r^-}{2} \quad (40)$$

An empirical anhysteretic model⁴ for piezoelectric material gives:

$$P_{an} = \frac{\gamma EP_s}{1 + \gamma E} \quad (41)$$

or

$$P_{an} = \frac{\sqrt{\beta} EP_s}{\sqrt{1 + \beta E^2}} \quad (42)$$

From the above two equations, one has:

$$\chi_{an1} = \frac{dP_{an}}{dE} = \frac{d}{dE} \left(\frac{\gamma EP_s}{1 + \gamma E} \right) \quad (43)$$

$$\gamma = \frac{-(2E_m \chi_{an} - P_s) + \sqrt{P_s^2 - 4 * P_s * E_m * \chi_m}}{2E_m^2 \chi_{an}} \quad (44)$$

$$\chi_{an1} = \gamma P_s$$

$$\chi_{an2} = \sqrt{\beta} P_s \quad (45)$$

as given by Smith and Ounaies⁴ and b is given as

$$b = -12P_s^2 \left[9E_m X_m - \sqrt{3} \sqrt{-4P_s^2 + 27E_m^2 \chi_m^2} \right] \quad (46)$$

Thus, χ_{an} can be approximated as

$$\chi_{an} = \frac{\chi_{an1} + \chi_{an2}}{2} \quad (47)$$

corresponding to initial slope.

4. RESULTS AND DISCUSSION

To illustrate the performance and prediction capabilities of the model and parameter estimation, one has considered the characterisation of hysteresis in a piezoelectric stack actuator developed using disc 5 PZT5H discs of diameter 6 mm and thickness 2 mm. Experimental displacement observations have been made from stack actuator for various input voltages between -500 V to +500 V from 2 kV switched mode power supply under free-stress condition using digital electronic gauge of 0.1 μ resolution. The corresponding field values have been calculated using the relation $E=V/h$, and have been used to predict hysteresis and resulting hysteretic E - P results. For the purpose, susceptibilities at various positions from the experimental data have been calculated and then the parameters have been determined using the formulae derived above. The various parameters used and the parameters estimated based on trial and error process are shown in Table 1. Actuator deflection in percentage of full-scale output with electric field is shown in Fig. 3, along with model values using estimated parameters for one set of observations. Model predictions are in close agreement with the experimental observations.

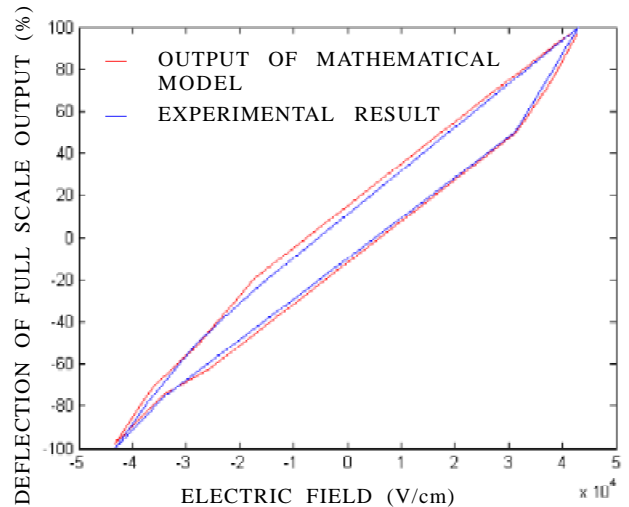


Figure 3. Comparison between predicted and experimental hysteresis behaviour between deflection and electric field of piezoelectric stack actuator.

Table 1. Various parameters used in model calculations and parameters estimated from model

Various parameters used in estimation		Estimated parameters
$\chi_r = 4.1928 \times 10^{-8}$	$\chi_{an1} = 5.8256 \times 10^{-8}$	$a = 1.0036 \times 10^4$
$\chi_m^+ = 6.3373 \times 10^{-8}$	$\chi_{an2} = 4.5357 \times 10^{-8}$	$\alpha = 0.904 \times 10^7$
$\chi_m^- = 4.2488 \times 10^{-8}$	$\chi_{an} = 5.1807 \times 10^{-8}$	$P_s = 2.505 \times 10^{-3}$
$\chi_m = 4.1920 \times 10^{-8}$	$\beta = 3.2785 \times 10^{-10}$	$k = 5000$
$\gamma = 2.3256 \times 10^{-5}$	$E_c = 5000$	$c = 0.9908$

5. CONCLUSION

The study characterises the inherent hysteresis in relationship with the input field and the output polarisation through quantification of the energy required to bend and translate domain wall pinned at inclusions in the material. This provides reversible and irreversible polarisation component whose sum represents the net polarisation due to the applied field. The flexibility of the model is further augmented by the small number of parameters (five) and their physical nature. For example, saturation polarisation (P_s) can be obtained directly from the data, the reversible coefficient (c) can be estimated from the ratio of slopes of polarisation curves at field reversal. Thus, the model uses susceptibilities at various locations on hysteresis graph to determine the unknown parameters. The accuracy of the obtained model parameters depends upon the degree to which slope information at initial, remanence, coercive and extreme points, quantifies the overall behaviour of the hysteresis curve. The model with parameters estimated, has been used to characterise PZT5H stack actuator. The model can easily be updated to accommodate the changing operating conditions often encountered in control applications.

ACKNOWLEDGEMENTS

Authors are thankful to Vice Chancellor, Defence Institute of Advanced Technology, Girinagar, Pune (MS), for granting permission to publish this work.

REFERENCES

- Croft, D. & Devasia, S. Hysteresis and vibration compensation for piezoactuators. *J. Guid. Cont. Dyna.*, 1998, **21**(5), 710-18.
- Singh, A.K. & Nagpal, P. Force-deflection behaviour of piezoelectric actuators. SPIE's International Symposium on Microelectronics and MEMS, 17-19 December 2001, Australia.
- Smith, R.C. & Hom, C.L. A domain wall model for ferroelectric hysteresis. *J. Intell. Mat., Syst. Struct.*, 1999, **10**(3), 150-61.
- Smith, R.C. & Ounaies, Z. A domain wall model for hysteresis in piezoelectric materials. *J. Intell. Mat., Syst. Struct.*, 2000, **11**, 62-79.
- Takacs, J. A phenomenological mathematical model of hysteresis. *Int. J. Comput. Math. Elec. Electr. Engg.*, 2001, **20** (4), 1002-014.
- Pulvari, C.F. & Kuebler, W. Phenomenological theory of polarisation reversal in $BaTiO_3$ single crystal. *J. Appl. Phys.*, 1958, **29**(9), 1315-321.
- Drougard, M.E. Detailed study of barium titanate. *J. Appl. Phys.*, 1958, **31**(2), 352-55.
- Landaure, R. Young, D.R. & Drougard, M.E. Polarisation reversal in barium titanate hysteresis loop. *J. Appl. Phys.*, 1956, **27**(7), 752-58.
- Nomura, S., Endo, M. & Kojima, F. Ferroelectric domains and polarisation reversal in $Pb(Zn_{1/3}Nb_{2/3})O_3$ crystal. *J. Appl. Phys.*, 1974, **13**(12), 2004-08.
- Pertsav, N.A. & Zembil'gotov, A.G. Microscopic mechanism of polarisation switching in polymer ferroelectrics. *Sovt. Phy. Solid State*, 1991, **33**(1), 165-71.
- Miller, R.C. & Savage, A. Motion of 180° domain walls in metal electrode barium titanate crystals as a function of electric field and sample thickness. *J. Appl. Phys.*, 1960, **31**(4), 663-69.
- Raghavan, A. Seshu, P. & Gandhi, P.S. Hysteresis modelling in piezoceramic actuator systems. *In Proceeding of the International Conference on Smart Materials, Structures and Systems*, 12-14, 2002, Bangalore.
- Hom, C.L. & Shankar, N. Modelling resonance tests for electrostrictive ceramics. *IEEE Trans. Ultra. Ferro. Freq. Cont.* 1999, 1422-429.

14. Jiles, D.C. & Atherton, D.L. Ferromagnetic hysteresis. *IEEE Trans. Magnetics*, 1983, Mag-**19**(5), 2183-185.
15. Fedosov, Sidorkin. Quasielastic displacement of domain boundry in ferroelectrics. *Sovt. Phys. Solid State*, 2001, **18**(6), 964-68.
16. Jiles, D.C. &. Atherton, D.L. Theory of magnetisation process in ferromagnets and its application to the magnetomechanical effect. *J. Phys. D: Appl. Phys.*, 1984, **17**, 1265-281.
17. Jiles, D.C.; Thoelke, J.B. & Devine, M.K. Numerical determination of hysteresis parameters for the modelling of magnetic properties using the theory of ferromagnetic hysteresis. *IEEE Trans. Magnet.*, 1992, **28**(1), 27-35.

Contributor



Dr A.K. Singh received his PhD from the University of Rajasthan, Jaipur, in 1992 and presently working in the Department of Instrumentation, Guided Missiles Faculty, Defence Institute of Advanced Technology, Girinagar, Pune. His areas of recent research interest include piezoelectric sensors, PC-based instrumentation, thermal sensors, laser instrumentation and smart materials. He has published more than 35 papers in various national and international journals.